JOURNAL OF MATERIALS SCIENCE **36** (2001) 123–129

Compositional effect on the crystallization of the cordierite-type glasses

YI HU, H.-T. TSAI
Department of Materials Engineering, Tatung University, Taipei, Taiwan
E-mail: huyi@ttu.edu.tw

The determination of apparent activation energies for the crystallization of P_2O_5/B_2O_3-containing cordierite-type glasses was conducted by non-isothermal differential thermal analysis (DTA). Glass with excesses both of SiO_2 and Al_2O_3 has a higher activation energy for crystallization. In addition to the main phase of α-cordierite, several other phases (farringtonite, clinoenstatite, and forsterite) were detected in the fully crystallized samples by the X-ray powder diffraction technique. The crystallization behavior for the powdered glass was governed by the surface crystallization mechanism, which would not change with composition.

1. Introduction

Cordierite ($Mg_2Al_4Si_5O_{18}$) based glass-ceramics have high potential of application in the electronic multilayer packaging because of their low dielectric constant and matching thermal coefficient of expansion to single crystal silicon [1–3]. As well known that the sintering process for packaging of the selected material is very important in successfully developing glass-ceramic/copper substrates with desired electrical, thermal, mechanical, and dimensional control properties. In forming the desirable glass-ceramic substrate materials, a unique sequence of events is required to occur in forming a useful substrate [4]. Complete densification of glass powder occurs at a temperature higher than 800°C, below which the carbon (e.g., from the decomposition of the binders) can be efficiently removed. Then the densified glass substrate would crystallize preferably around 900 to 950°C in order to be cofired with copper [4]. Through the formation of low-expansion α-cordierite as the dominating crystal phase and small amount of second phase, a proper thermal-expansion match to single-crystal silicon can be achieved [4]. Therefore, to optimize the sinterability of the glass-ceramic materials, it is essential to know the crystallization behavior of the glasses.

In the sintering of cordierite glass powders, nucleation agents are not necessary present in the glass composition because crystallization can generally take place by nucleation from the surface of the original particle. It was found that glass powders of the stoichiometric cordierite composition are difficult to densify owing to their very narrow sintering range crystallization stops the sintering [5]. Improving the sinterability of stoichiometric cordierite glass powders involves either (1) the change of glass composition with more MgO and less Al_2O_3 or (2) the addition of sintering aids such as P_2O_5 and B_2O_3 [1, 6].

Crystallization mechanisms of α-cordierite precipitated from bulk and powdered glasses have been extensively studied in the past [7–12]. For example, Amista *et al.* [9] studied the influence of the cordierite primary composition on the phase formation. Watanabe and Giess [8, 9] prepared the glass composition of $MgSiO_3$-rich cordierite modified with small amount (<0.5%) of P_2O_5 and B_2O_3 for crystallization investigation. Rudolph *et al.* [12] studied the effect of P_2O_5 on the crystallization activation energy of the cordierite-type glass. Donald [12] has reported detailed thermal analysis of the crystallization kinetics of the cordierite glass. However, the effect of the constituent on the crystallization behavior of cordierite-type glasses has not been evaluated.

Detailed knowledge based on the chemical composition is essential for the industries, although the effect of chemical composition on the glass properties and crystallization might be predicted. On the other hand, although a number of studies have been reported aimed specifically at examining the sintering and/or crystallization mechanisms of cordierite-bases glasses [13–20], a more comprehensive data base is required before a clearer understanding of the crystallization processes can emerge.

In the present investigation, we are interested in understanding the crystallization behavior of the glasses with the composition in the primary cordierite phase field containing small amount of P_2O_5 and B_2O_3. The crystallization kinetics of the glass was determined by means of non-isothermal DTA.

2. Experimental procedure

The glass composition studied lies in the cordierite primary phase field and all the samples containing additional 2.5wt%P_2O_5 and 2.5wt%B_2O_3 (Table I). These glasses are distributed into three groups with excess of one or two of the three components, MgO, Al_2O_3 and SiO_2. Glasses were obtained by melting a homogeneous mixture of regent-grade $Mg(OH)_2$, SiO_2, Al_2O_3, B_2O_3 and H_3PO_4 at 1550°C for 4 hours in a Pt crucible.

TABLE I Composition and properties of the MgO-Al_2O_3-SiO_2 glasses ($\phi = 10$°C/min). The stoichiometric composition is MgO : Al_2O_3 : SiO_2 = 22 : 22 : 56. Additional 2.5 wt%P_2O_5 and 2.5wt%B_2O_3 were added in the glasses

Sample No.	Composition(mol%) MgO:Al_2O_3:SiO_2	T_g (°C)	T_c (°C)	T_p (°C)	$T_c - T_g$ (°C)
A1	23 : 20 : 57	885	993	1025	108
A2	23 : 21 : 56	884	985	1012	101
A3	23 : 22 : 55	883	981	1009	98
A4	23 : 23 : 54	880	980	1009	100
B1	24 : 22 : 54	876	975	1000	101
B2	23 : 23 : 54	880	980	1009	100
B3	20 : 26 : 54	885	988	1005	103
B4	18 : 28 : 54	890	1002	1023	108
C1	19 : 21 : 60	896	987	1011	91
C2	21 : 21 : 58	888	986	1015	98
C3	23 : 21 : 56	884	985	1012	101
C4	24 : 21 : 55	877	981	1016	105

T_g = glass transition temperature, T_c = crystalllization temperature, T_p = ppeak temperature (as indicated in Fig. 1).

The melt with the Pt crucible was quenched into distilled water into the form of bulk beads. On the other hand, bulk glass was obtained by pouring the melt into a steel mold. These glass beads and bulk glass (with steel mold) were annealed at 500°C for one hour and cooled in the furnace. Glass powders were obtained by wet-ball milling the glass beads for 24 hours in PE bottles containing yttria-stabilized zirconia balls and alcohol. The average particle sizes of the resulting glass powders were measured with a particle size analyzer (Model MSE02SM, Malvern Instruments Ltd.) and were in the range of 2.5–5 μm. Non-isothermal crystallization kinetics of the glass powders was studied using a Dupont TA-2000 system. All the powdered samples were subjected to the same conditions for kinetic analysis: heating rate $\phi = 10$, 15, 20, 25°C/min and purge air flux = 20 cm^3/min.

Viscosity measurements were made using a beam-bending viscometer (Theta 7300). The viscosity was determined by measuring the rate of midpoint deflection of a simply loaded glass beam in the 850 to 920°C temperature ranges. Samples of size 0.445 cm (height) × 0.610 cm (width) × 4.180 cm (length) were cut from the annealed bulk glass. The span used was 3.125 cm. The operation followed ASTM procedure [21] and isothermal data was taken [22].

The glass powders were granulated with 5 wt% poly(vinyl alcohol) (PVA) and then were pressed into discs under a uniaxial pressure of 100 MPa. Glass-ceramic samples were obtained by isothermal heat treatments of the disc samples at 900°C in air. Phase evolution in these disc samples was investigated by X-ray powder diffraction using Cu-K_α radiation. The crystallized samples were polished and given a light etch with 2.5 M HF for 30 seconds. The morphologies of the etched samples were examined by the scanning electron microscopy (SEM).

3. Results and discussion

3.1. Thermal properties of the glasses

Mean values for the DTA characteristic temperatures of the glass powder with heating rate of 10°C/min are summarized in Table I. Only one signal of exothermic peak was observed for all samples from DTA scans in the temperature range from 100 to 1000°C. Glass transition temperature, T_g, has been taken in the present work as the extrapolated start and the extrapolated end of the transition peak as in Fig. 1. The crystallization exotherm, Tc, is characterized by the exothermic peak with a low temperature shoulder. It was found that T_g decreased with the increasing ratio of Al_2O_3/SiO_2 in the group A glasses, MgO/Al_2O_3 in group B glasses, and MgO/SiO_2 in group C glasses.

The viscosity data of three glass samples obtained as a function of temperature are shown in Fig. 2. It has been known that viscosity represents one of the most important properties for a quantitative interpretation of the crystallization process. Numerous treatments of glass viscosity as a function of temperature and composition

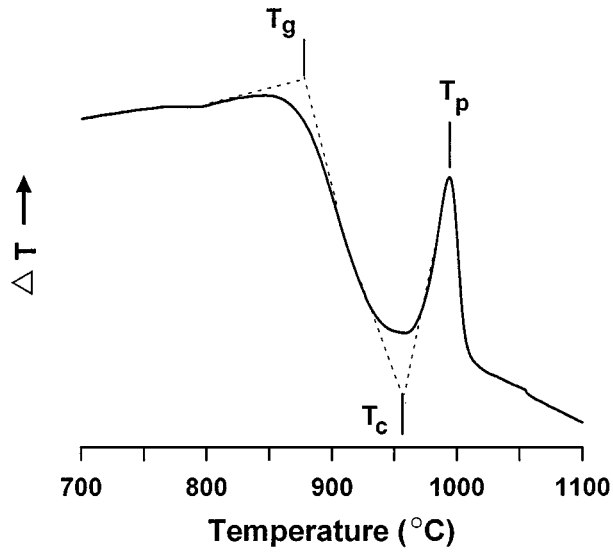

Figure 1 Typical DTA curve of the glass with the heating rate of 10 °C/min.

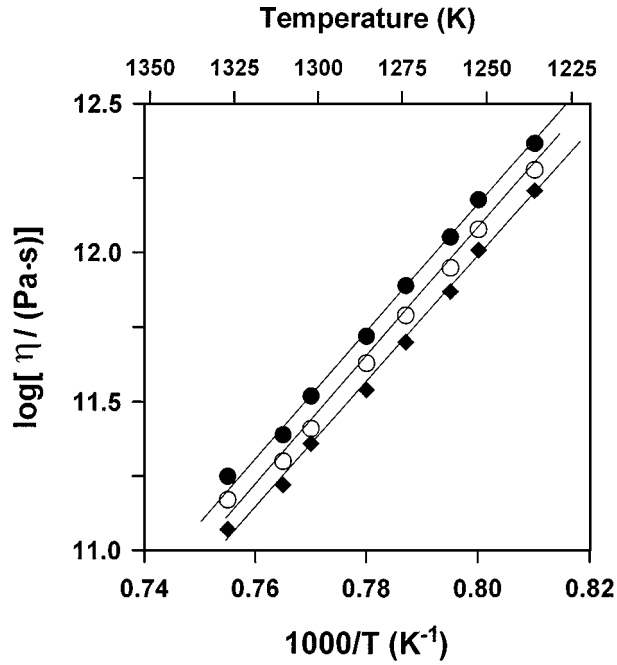

Figure 2 Viscosity behavior of A3(○), B2(♦), and C2(●) glasses determined by beam-bending method.

have been made [23]. An Arrhenius-type equation was applied to obtained the activation energy (E_η) for viscous flow for a short temperature range:

$$\log \eta = \log \eta_o + \frac{E_\eta}{2.3RT} \tag{1}$$

where η_o is a constant, R is the gas constant, and T is the absolute temperature. The average value of E_η was determined to be about 411 kJ/mol by a least square fit of $\log \eta$ versus the reciprocal temperature from measurements of these glass samples as in Fig. 2. Since the slopes for these glasses are very close, the activation energy is assumed to be a constant for all composition. Besides, the addtivity of constituent contribution to the value of η_o is also assumed. The assumptions and the determination of viscosity coefficients corresponding to the effect of additivity of constituent for the same glass system have been conducted by Geiss and Knickerbocker [24]. Here, we adapt another way to portray the relationship between viscosity and temperature. The viscosity at the glass transition temperature (T_g) is assumed to be constant and the viscosity coefficients are determined by introducing T_g into Equation (1).

$$\log \eta(T_g) = [m][Cv] + E_\eta/2.3RT_g \tag{2}$$

where [m] and [Cv] are the matrixes of the constituents (in molar ratio) and viscosity coefficients, respectively. It was found that the viscosity at T_g, which obtained form the non-isothermal DTA measurement, is about $10^{13.5}$ Pa·s.

The computed viscosity coefficients, Cv, were $-0.0.093$ -0.0555, and -0.0322 for MgO, Al_2O_3 and SiO_2, respectively. The largest difference between a calculated and a measured T_g was less than 3 degrees. Fig. 3 shows the effect upon of adding up to 10 mole% of each constituent in turn to the stoichiometric cordierite composition according to Equation 2 and confirms that MgO lowers T_g most while SiO_2 increases T_g slightly and Al_2O_3 has the least effect on T_g.

The effect of each constituent on the viscosity of the glass can be explained by the number of non-bridging oxygen in the glass network. Since the glass transition temperature (T_g) mainly depends on the strength and connectivity of the glass network, the structure change caused by increasing MgO, which acts as a modifier, will thus result in a decrease in T_g as in group B and C glasses (Table I). In the silicate glasses, Al^{3+} is believed to coexist with four and six coordination numbers [25]. The shortage of oxygen from the network construction by [AlO_4] would convert the non-bridging oxygen to bridging oxygens owing to valence compensation. However, [AlO_6] would behave more like a modifier and cause a loose in glass network. The effect of [AlO_4] unit on the increase of T_g would be lowered by the [AlO_6] unit.

3.2. Nucleation

The procedure, which can be used for the determination of nucleation rates via DTA experiments, has been described by Ray and Day [26]. Typical DTA crystallization exotherms with different heating rate are shown in Fig. 4. Here, the nucleation rate was determined by the peak position method that the variation of T_p with nucleation temperature could be employed for the computation of the temperature dependence of the nucleation rate. Using either the isothermal Johnson-Mehl-Avrami equation [27] or the modified non-isothermal solid-state phase transformation theory [28] leads to a relationship between the T_p and the number of nuclei per unit volume, N, in a glass as

$$\ln N(T_n) = \ln \phi + \frac{E}{RT_p} + \text{constant} \tag{3}$$

where ϕ is the heating rate, E is the activation energy for crystal growth, and T_n is the nucleation temperature. The value of N is assumed proportional to the nucleation temperature. Fig. 5 shows the relationship for the A3 glass nucleated at different temperature for 3 h. It was found that the value of $1/T_p$ is essen-

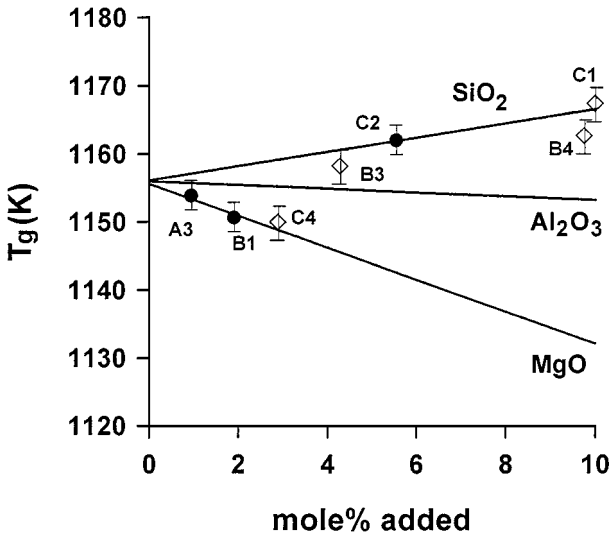

Figure 3 The effect of each constituent upon glass transition temperature as calculated using Equation 2. Some data points are also shown in the figure. ●: Glass with nearly one excess constituent. ◇: Glass with two excess constituents.

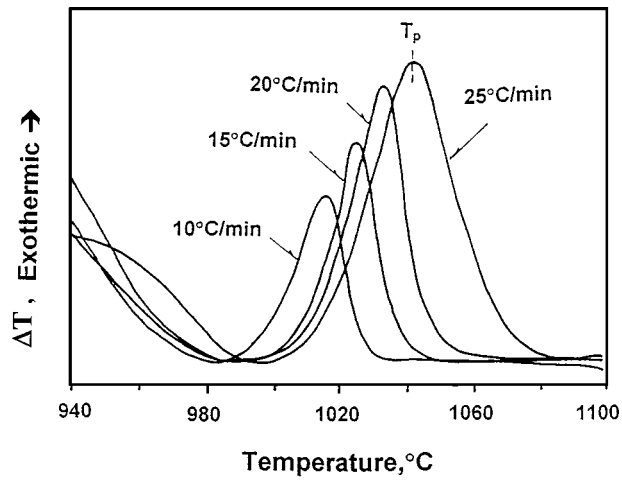

Figure 4 Typical DTA crystallization exotherms for the C2 glass with different heating rate.

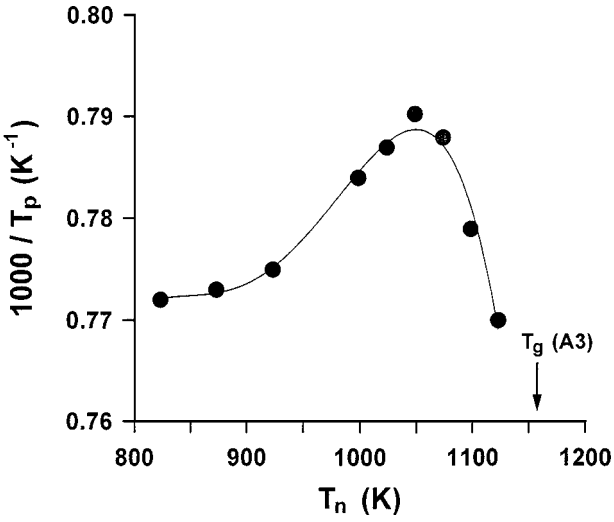

Figure 5 Inverse of T_p for the A3 glass as a function of the nucleation temperature (T_n). T_p was obtained from the DTA-curve with the heating rate of 10 °C/min.

tially constant until the glass is nucleated above 700°C. Fig. 5 further shows that the temperature where the nucleation can occur in the A3 glass ranges from 700 to 850°C and the maximum nucleation rate helds at $T_{max} = 815 \pm 10$°C.

Zanotto shows that, for homogeneous nucleation, the calculated values of T_{max} are also close to T_g, in agreement with James's observations; it was also demonstrated that the reverse also applies, ie. if the predicated T_{max} falls below T_g, only surface (heterogeneous) nucleation is observed [29, 30]. In the present study, crystallization behavior of the cordierite-type glass might be classified as surface nucleation since its T_{max}(∼815°C) is somewhat below T_g (∼880°C). This confirms the observations by other people who have demonstrated that the crystallization for the cordierite-type glasses occurs from the glass surface toward the inside by the surface-nucleation mechanism [11, 12, 31]. As we know that Zanotto and James dealed with stoichiometic crystallization only. The failure of the present glasses with low T_{max} to crystallize homogeneously may be attributed to their particular small steady state nucleation rate [29]. Non-stoichiometic composition and other factors (e.g., secondary phases, phase separation,..) can have the influence on the nucleation rate.

3.3. Crystallization kinetics

The crystallization kinetic parameters were evaluated by means of the thermoanalytical techniques based on the well-known equation [32, 33]:

$$\ln\left(T_p^2/\phi\right) = \ln\left(\frac{E_c}{R}\right) - \ln \nu + \frac{E_c}{RT_p} \qquad (4)$$

where T_p is the peak temperature of the crystallization exoterm, ϕ is heating rate, E_c is the activation energy for crystallization. This equation is based on the Johnson-Mehl-Avrami isothermal kinetic model [34, 35], which was extended for use in non-isothermal methods by Augis and Bennett for surface crystallization ($n = 1$) [36]. A plot of $\ln(T_p^2/\phi)$ vs. $1/T_p$ should be a straight line, from which the activation energy, E_c, and the frequency factor, ν, can be determined from the slope and intercept, respectively.

The corresponding non-isothermal activation energy plots of group A glasses from Equation 2 are shown in Fig. 6. The values of the activation energies and frequency factors for crystallization of all glass samples by the non-isothermal methods are summarized in Table II. It is found that the activation energy increases significantly with the decreasing ratio of MgO/Al_2O_3 in group B glasses and MgO/SiO_2 in group C glasses, whereas only a small variation of E was observed in group A glasses. Similar trend in the variation of frequency factor was observed in these glasses.

To reconfirm the surface crystallization mechanism for present glasses, values of the Avrami parameter (n) were evaluated from the non-isothermal data using an expression derived by Piloyan *et al.*: [37]

$$\frac{\mathrm{d}[\ln(\Delta y)]}{\mathrm{d}(1/T)} = -\frac{nE}{R} \qquad (5)$$

where (Δy) is the vertical displacement at temperature T of the DTA crystallization exotherm from the baseline. Equation 5 is valid only when the crystallized volume is less than 0.2. The corresponding Avrami constant plots of group A glasses from Equation 5 are shown in Fig. 7 and the values of Avrami constant were given in Table II. The crystallization mechanism of cordierite is verified as surface crystallization mechanism with the n value of near 1

Clearly the difference in the crystallization parameters apparently arises from the variation of the chemical composition. The overall activation energies in the present study are in the range 397–506 kJ/mol. Comparison with the cordierite glass, the crystallization rate of some aluminosilicate glasses has been reported to be relatively slow and mass transport through the glass to the growing interface is usually rate-controlling [8, 10]. As the crystal front grows into the glass, it rejects any impurities or excess constituent into intercrystalline

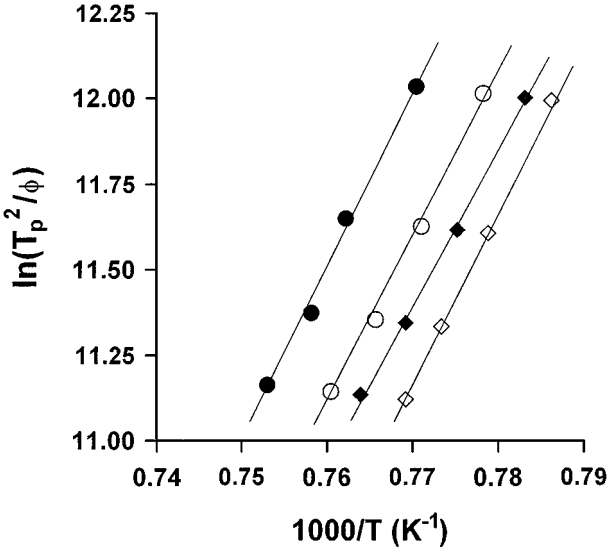

Figure 6 The plot of $\ln(T_p^2/\phi)$ versus the reciprocal crystallization peak temperature, T_p. ●:X = A1, ○ :X = A2, ♦:X = A3, ◇:X = A4

TABLE II Crystallization kinetic parameters for the glasses as determined by non-thermal DTA

Sample No. (Excess component)	$E_c^{\#}$ (kJ mol^{-1})	Frequency factor ν (sec^{-1})	Avrami parameter* n
A1 (Mg,Si)	425	3.7×10^{13}	1.1
A2 (Mg,Si)	411	1.6×10^{13}	1.2
A3 (Mg,Al)	409	1.4×10^{13}	1.0
A4 (Mg,Al)	404	1.2×10^{14}	1.1
B1 (Mg,Al)	378	8.5×10^{11}	1.3
B2 (Mg,Al)	404	1.2×10^{14}	1.1
B3 (Al,Si)	487	2.7×10^{17}	1.2
B4 (Al,Si)	506	8.2×10^{18}	1.2
C1 (Al, Si)	465	6.3×10^{17}	1.2
C2 (Si)	422	1.7×10^{14}	1.1
C3 (Mg,Si)	411	1.6×10^{13}	1.3
C4 (Mg, Si)	389	4.2×10^{12}	1.0

#:±5kJ/mol *:±0.2.

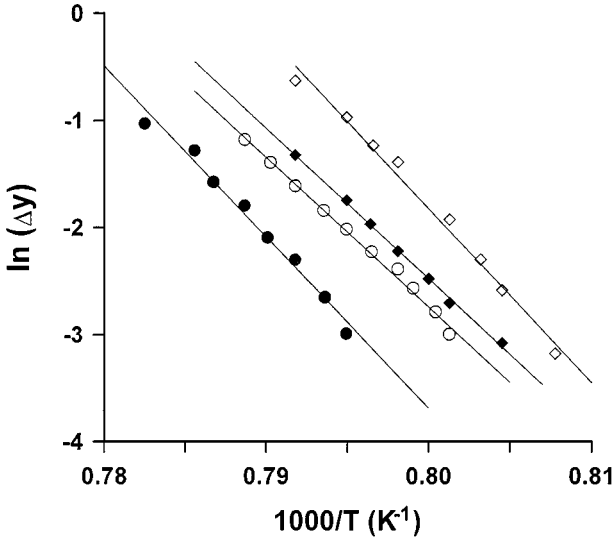

Figure 7 The plot of $\ln(\Delta T)$ against $1/T$ for $\phi = 10\,^{\circ}$C/min. ●:X = A1, ○ :X = A2, ♦:X = A3, ◇:X = A4

regions. Since Si^{4+} and Al^{3+} ions have higher field strength and large ionic size than Mg^{2+} ion, it should be more difficult to reject Si^{4+} or Al^{3+} ion than reject Mg^{2+} from the crystal front. Besides, the glass structure becomes more connective and rigid with increasing the amount of Si^{4+} and Al^{3+} ions. The latter can largely decrease the number of non-bridging oxygen by forming [AlO_4] unit. The relative high activation energies of sample B3, B4 and C1, therefore, are attributed to the excess of both Si^{4+} and Al^{3+} ions, the network formers. On the other hand, the relative low activation energies of B1 and C4 are from the excess MgO in the glass matrix. Much comparative low activation energies of crystallization obtained by Rudolph *et al.* and Watanabe *et al.*, therefore, are attributed to the considerable excess of MgO [8, 11].

3.4. Crystallization phases

Fig. 8 shows the microstructure of the compacted glass A1 heated at 900°C for different duration. Typical cellular growth of α-cordierite is observed that comes from the interface-controlled diffusion process. The interfacial boundaries between the crystal and glass matrix have been etched more heavily than other regions. These boundaries are examined to be the surfaces of the original glass particles.

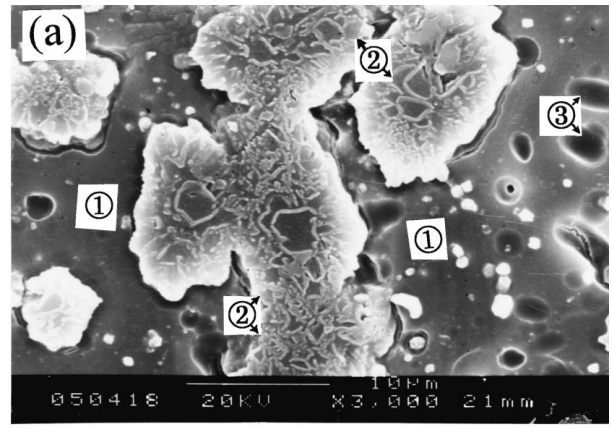

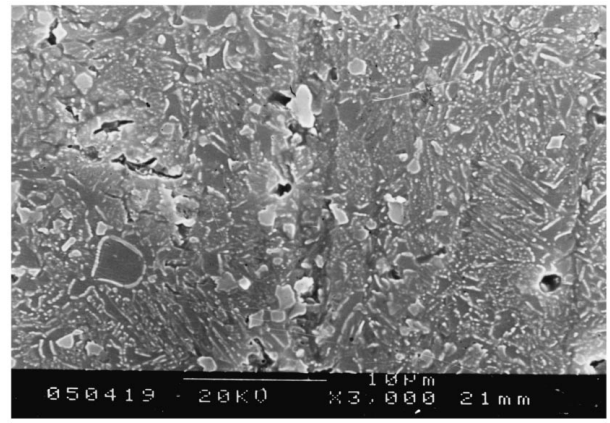

(b)

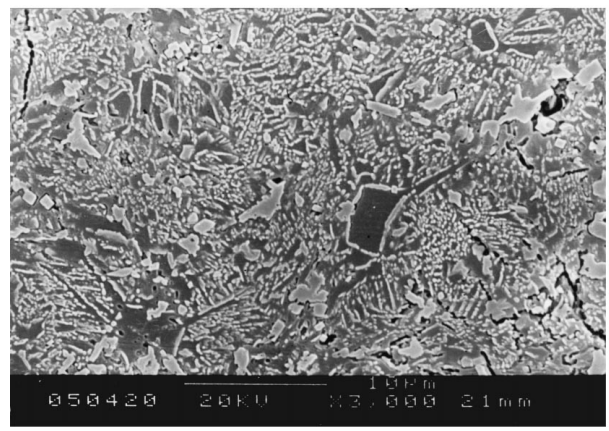

(c)

Figure 8 SEM photographs of A1 glass heat treated at the 900°C for (a) one hour, (b) three hours, (c) four hours. ①: glass, ②: cellular grain, ③: pore.

Fig. 9 shows the typical X-ray powder diffraction patterns of the glass sample A1, heat treated at different temperature. Phases were identified using JCPDS cards 13-293 for a-cordierite, 25-1372 for farringtonite ($3MgO{\cdot}P_2O_5$), 19-769 for clinoenstatite ($MgSiO_3$), and 21-1260 for forsterite (Mg_2SiO_4). These phases all precipitate at the initial stage of crystallization as observed at lower annealing temperature (~850°C). However, α-cordierite became to be the main crystalline phase at higher temperatures (900 and 950°C).

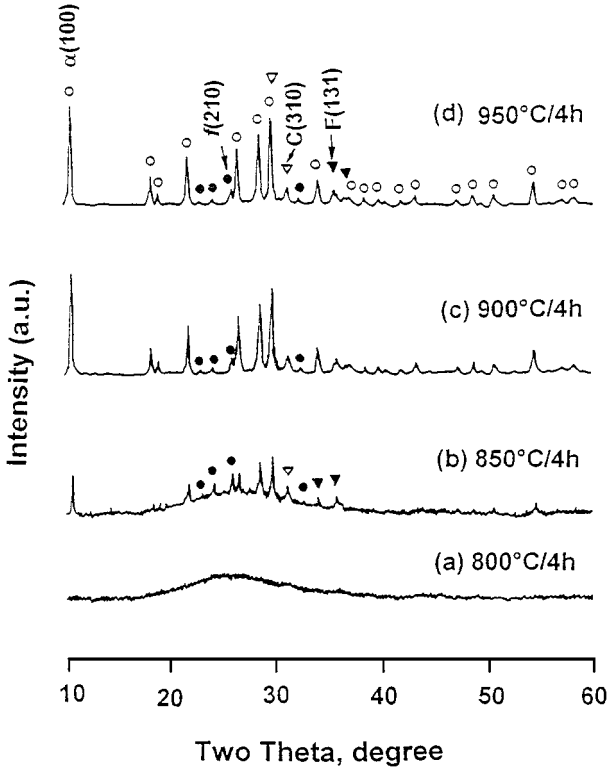

Figure 9 XRD powder spectra showing the phase evolution of the glass sample A1 heated at 950°C for four hours. ○ : α-cordierite, ●:farringtonite, ∇:clinoenstatite, and ▼ : forsterite.

Table III shows the relative intensity of the representative peak of each phase to α-cordierite phase for the samples heated at 950°C. It is found that the relative intensity of farringtonite phase is nearly independent on the composition of the glass. On the other hand, both the relative intensities of clionenstatite and forsterite phases decrease with the increasing ratio of Al_2O_3/SiO_2 in group A glasses, Al_2O_3/MgO in group B glasses, and SiO_2/MgO in group C glasses. The volumes of these minor phases after crystallization process are associated with the constituent of glass. Excess Mg and Si in the glass would favor the formation of Mg-Si-O based phases such as clinoenstatite and forsterite crystals as seen in Table III. The limitation of the formation of farringtonite phase is due to the definitively small amount of P_2O_5 in the glass. Though the volume fraction of the second phases seems not to affect the activation energy and the Avrami parameter apparently, the results are thus the effective parameters (T_p, Ec,...) of a complex crystallization process.

It is found that farringtonite, clinoenstatite, and forsterite precipitate with comparative volume to α-cordierite at lower annealing temperature (850°C) as in Fig. 9. The relative volumes of these phases to α-cordierite phase become much smaller at higher heating temperatures ($T \geq 900$°C). This indicates that the formation of these minor phases is confined in a certain degree in the crystallization process. It has been reported that P_2O_5/B_2O_3 containing cordierite glass consists of heterogeneous nucleation sites left at the position of the surface of the particles and to form the pellet and cellular growth of α-cordierite [14]. The formation of these minor phases at initial heat treatment stage might result from the cellular growth of α-cordierite. As the crystal front grows into the glass, it rejects any impurities such as P_2O_5 and B_2O_3 and excess constituent elements into the intercrystalline regions. Therefore, minor phases such as farringtonite, clinoenstatite, and forsterite would form at the intercrystalline regions.

TABLE III Relative intensity of the crystallized phases in the samples which was heat treated at 950°C for 4 hours

Sample No. (excess component)	$I_{f(100)}/I_{\alpha(100)}$	$I_{C(310)}/I_{\alpha(100)}$	$I_{F(131)}/I^*_{\alpha(100)}$
A1(Mg,Si)	0.05	0.25	0.22
A2(Mg,Si)	0.04	0.23	0.19
A3(Mg,Al)	0.04	0.08	0.09
A4(Mg,Al)	0.03	0.05	0.06
B1(Mg,Al)	0.04	0.08	0.09
B2(Mg,Al)	0.04	0.05	0.06
B3(Al,Si)	0.02	0.02	0.04
B4(Al,Si)	0.02	<<0.01	<<0.01
C1(Al,Si)	0.02	0.07	0.05
C2(Si)	0.02	0.11	0.10
C3(Mg,Si)	0.04	0.23	0.19
C4(Mg,Si)	0.05	0.24	0.23

α:α-cordierite, f:farringtonite, C:clinoenstatite, F:forsterite, *accuracy in ±5%.

4. Summary

Crystallization kinetics of P_2O_5/B_2O_3-containing cordierite based glass powder was studied by non-isothermal differential thermal analysis (DTA). The crystallization mechanism of the cordierite-type glass powder was governed by surface crystallization from the origin particle surfaces based on the n values of near one. α-cordierite with several minor phases (farringtonite, clinoenstatite, and forsterite) were detected in the annealed samples. The XRD results show the effective parameters to be of a complex crystallization process. Cellular crystal growth morphologies of α-cordierite crystals in the glass observed by SEM.

Acknowledgment

The work report herein was supported by National Science Council, the Republic of China, under contact No. NSC84-2216-E-036-018.

References

1. S. H. KNICKERBOCKER, A. H. KUMAR and L. W. HERRON, *Am. Ceram. Soc. Bull.* **72** (1993) 90.
2. G. PARTRIDGE, C. A. ELYARD and H. D. KEATMAN, *Glass Technol.* **30** (1989) 215.
3. S. H. KNICKERBOCKER, *Am. Ceram. Soc. Bull.* **71** (1992) 1393.
4. R. R. TUMMALA, *J. Am. Ceram. Soc.* **74** (1991) 895.
5. R. MORRELL, *Proc. Br. Ceram. Soc.* **28** (1979) 53.
6. A. H. KUMAR, P. W. McMILLAN and R. R. TUMMALA, U.S. Patent 4 301324 (1981).
7. K. WATANABE and E. A. GIESS, *J. Am. Ceram. Soc.* **68** (1985) C102.
8. *Idem., J. Non-Cryst. Solids* **169** (1994) 306.
9. P. AMISTA, M. CESARI, A. MONTENERO, G. GNAPPI and L. LAN, *ibid.* **192 & 193** (1995) 529.

10. A. G. GREGORY and T. J. VERSEY, *J. Mater. Sci.* **6** (1971) 1312.
11. T. RUDOLPH, W. PANNHORST and G. PETZOW, *J. Non-Cryst. Solids* **155** (1993) 273.
12. I. W. DONALD, *J. Mater. Sic.* **30** (1995) 904.
13. Y. HIROSE, H. DOI and O. KAMIGAITO, *J. Mater. Sci. Lett.* **3** (1984) 153.
14. D. R. BRIDGE, D. HOLLAND and P. W. McMILLAN, *Glass Technol.* **26** (1985) 286.
15. M. A. McCOY and A. H. HEUER, *J. Am. Ceram. Soc.* **67** (1986) 292.
16. T. I. BARRY, J. M. COX and R. MORRELL, *J. Mater. Sci.* **23** (1978) 1534.
17. M. AWANO, H. TAKAS and Y. KUWAHARA, *J. Am. Ceram. Soc.* **35** (1992) 2535.
18. M. GLENDENNING and W. E. LEE, *ibid.* **79** (1996) 705.
19. E. A. GIESS, J. P. FLETCHER and L. W. HERRON, *ibid.* **67** (1984) 549.
20. R. CHAIM and A. H. HEUER, *ibid.* **75** (1992) 1512.
21. ASTM Designation C598-72, Annual Book of ASTM Standards, Part 17 (American Society for Testing and Materials, Philadelphia, 1973) p. 552.
22. R. J. LOCKER, B. S. thesis, Alfred University, Alfred, NY, 1980.
23. H. SCHOLZE and N. J. KREIDL, in "Glass Science and Technology, Vol. 3: Viscosity and Relaxation," edited by D. R. Uhlmann and N. J. Kreidl (Academic Press, New York, 1986).
24. E. A. GEISS and S. H. KNICKERBOCKER, *J. Mater. Sci. Lett.* **4** (1985) 835.
25. B. E. YOLDAS, *Phys. Chem. Glasses* **12** (1971) 28.
26. C. S. RAY and D. E. DAY, *J. Am. Ceram. Soc.* **73** (1990) 439.
27. A. MAROTTA, A. BURI and G. L. VALENTI, *J. Mater. Sci.* **13** (1978) 2483.
28. X. XU, J. LI and L. YAO, *J. Shanghai Inst. Build. Mater.* **2** (1989) 104.
29. P. F. JAMES, *J. Non-Cryst. Solids* **73** (1985) 517.
30. E. D. ZANOTTO, *ibid.* **89** (1987) 361.
31. K. WATANABE, E. A. GIESS and M. W. SHAFER, *J. Mater. Sci.* **20** (1985) 508.
32. N. P. BANSAL and R. H. DOREMUS, *J. Therm. Anal.* **29** (1984) 115.
33. H. E. KISSINGER, *Anal. Chem.* **29** (1957) 1702.
34. W. A. JOHNSON and R. F. MEHL, *Trans. Amer. Inst. Elec. Eng.* **135** (1939) 416.
35. M. AVRAMI, *J. Chem. Phys.* **9** (1941) 177.
36. J. A. AUGIS and J. D. BENNETT, *J. Thermal. Anal.* **13** (1978) 283.
37. G. O. PILOYAN, I. D. RYBACHIKOV and O. S. NOVI, *Nature* **212** (1960) 303.
38. B. H. MUSSLER and M. W. SHAFER, *Am. Ceram. Soc. Bull.* **64** (1985) 1459.

Received 14 October 1999
and accepted 22 May 2000